

General localization lengths for two interacting particles in a disordered chain

Pil Hun Song and Felix von Oppen

Max-Planck-Institut für Kernphysik, Postfach 103980, D-69029 Heidelberg, Germany

(Received 1 July 1998)

The propagation of an interacting particle pair in a disordered chain is characterized by a set of localization lengths that we define. The localization lengths are computed by a new decimation algorithm and provide a comprehensive picture of the two-particle propagation. We find that the interaction delocalizes predominantly the center-of-mass motion of the pair and use our approach to propose a consistent interpretation of the discrepancies between previous numerical results. [S0163-1829(99)13501-X]

The problem of interacting electrons in a disordered potential is one of the important unsolved problems in condensed-matter physics. This has been emphasized again by the recent observation¹ of a metal-insulator transition in two-dimensional (2D) systems that was not anticipated theoretically. Some time ago, Shepelyansky² proposed that it would be worthwhile to consider the simple case of two interacting particles in a random potential. By an approximate mapping of the problem to a random banded matrix model, he predicted that unexpectedly, such a particle pair could propagate coherently over distances ξ_2 much larger than the single-particle localization length ξ_1 as long as the two particles are within ξ_1 from each other. After Shepelyansky, many authors³⁻⁷ have tried to obtain more rigorous results. However, at the present stage, there exists a controversy not only over the expression³⁻⁶ for ξ_2 but even over the existence of the enhancement effect itself.^{7,8} Our purpose in this paper is to present a more comprehensive picture of the two-particle propagation by defining and computing a set of localization lengths. We unambiguously show that the effect exists and propose a resolution of the controversy in the previous studies.^{7,8}

Specifically, Shepelyansky obtained for the two-particle localization length

$$\xi_2 \sim (U/W^2)^2, \quad (1)$$

where U denotes the interaction strength and W the disorder strength. Since $\xi_1 \sim 1/W^2$, Eq. (1) implies an enhancement of the localization length for weak disorder. Since Shepelyansky's original argument involved several uncontrolled assumptions for the single-particle eigenstates, a number of (mostly numerical) attempts³⁻⁷ to refine the result followed afterwards. Imry³ rederived Shepelyansky's result, Eq. (1), by an extension of the Thouless block scaling picture. Frahm *et al.*⁴ computed $\xi_2 \sim W^{-3.3}$ using the transfer-matrix method (TMM). von Oppen *et al.*⁵ introduced a Green's function approach, allowing one to project the problem on the subspace of doubly occupied sites, and concluded $\xi_2 \sim U/W^4$. Subsequently, Song and Kim⁶ treated the idea of von Oppen *et al.* rigorously using the recursive Green's function method and found $\xi_2 \sim W^{-2.9}$. Recently, Römer and Schreiber⁷ suggested from the TMM result that the enhancement effect does *not* exist.

It is currently not clear whether these ideas have any relevance to the degenerate finite-density Fermi gas. It appears to be the most promising direction to consider the localization properties of quasiparticle pairs. There have been a number of studies^{3,9,10} of whether quasiparticle excitations delocalize relative to single-particle ones. While a numerical study for a one-dimensional (1D) system showed delocalization only for unrealistically high excitation energy of the pair (of order of the bandwidth),⁹ both arguments³ and numerical studies¹⁰ in higher dimensions suggest the possibility of a new pair mobility edge close to the ground state.

The two-particle problem in one-dimension is described by the Hamiltonian

$$\mathcal{H} = H_1 \otimes \mathbf{1} + \mathbf{1} \otimes H_1 + U \sum_m |m\rangle |m\rangle \langle m| \langle m|, \quad (2)$$

where m labels the N sites of the 1D lattice and H_1 is the usual single-particle Anderson Hamiltonian

$$H_1 = \sum_m [\epsilon_m |m\rangle \langle m| + t(|m\rangle \langle m+1| + |m+1\rangle \langle m|)]. \quad (3)$$

ϵ_m is a random-site energy, drawn from a box distribution with $-W/2 \leq \epsilon_m \leq W/2$, and U the on-site interaction. The hopping matrix element t is set to unity throughout this work. A convenient quantity to study the localization properties of the pair is the two-particle Green's function $G = (E - \mathcal{H})^{-1}$. The two-particle localization length ξ_2 on which previous studies have focused is defined in terms of G as⁵

$$\xi_2^{-1} = - \lim_{|n-m| \rightarrow \infty} \frac{1}{|n-m|} \langle \langle \ln |\langle m, m | G | n, n \rangle| \rangle \rangle, \quad (4)$$

where the double bracket denotes the disorder average.

In this paper, we discuss general localization lengths that provide a much more comprehensive picture of the localization properties of the particle pair. First, we consider a general center-of-mass (CM) motion by defining

$$\xi_{2,a}^{-1} = - \lim_{|n-m| \rightarrow \infty} \frac{1}{|n-m|} \langle \langle \ln |\langle m, m-a | G | n, n-a \rangle| \rangle \rangle. \quad (5)$$

We find that, surprisingly, $\xi_{2,a}$ is essentially independent of the particle distance a , even if a exceeds the single-particle

localization length ξ_1 . We also study the behavior of G for relative motion at fixed CM, as characterized by

$$\xi_r^{-1} = - \lim_{n \rightarrow \infty} \frac{1}{n} \langle \langle \ln | \langle m+n, m-n | G | m, m \rangle | \rangle \rangle. \quad (6)$$

Finally, we consider the propagation of one of the particles with the other held fixed, as described by

$$\xi_f^{-1} = - \lim_{n \rightarrow \infty} \frac{1}{n} \langle \langle \ln | \langle m, m+n | G | m, m \rangle | \rangle \rangle. \quad (7)$$

As opposed to ξ_2 and $\xi_{2,a}$, we find that the latter two lengths are only very weakly affected by the interaction U . Nevertheless, it will turn out that these lengths are indispensable for obtaining a more comprehensive picture of the two-particle propagation and for understanding the discrepancies between previous numerical results.

While ξ_2 could be computed by projecting the problem on the subspace of doubly occupied sites, this is no longer possible for the generalized localization lengths defined above. For this reason, we introduce a new decimation algorithm, which allows us to compute these localization lengths efficiently. As opposed to the projection method for ξ_2 used in Ref. 5, this algorithm is numerically exact. We briefly describe the procedure for computing ξ_2 . Adaption to the other lengths defined above is straightforward. Since the interaction acts only on symmetric states, we specify to (spinless) bosons. Using a symmetrized basis

$$|mn\rangle = \begin{cases} |m\rangle|m\rangle & \text{if } m=n, \\ (1/\sqrt{2})(|m\rangle|n\rangle + |n\rangle|m\rangle) & \text{if } m \neq n, \end{cases} \quad (8)$$

and interpreting (m,n) as sites of a 2D square lattice, the Hamiltonian of Eq. (2) can be interpreted as describing a single particle on the 2D lattice shown by the thin solid lines in Fig. 1. The off-diagonal elements of \mathcal{H} are nonzero only for nearest-neighbor bonds and equal to $\sqrt{2}$ (1) if one (none) of the nearest-neighbor sites is a doubly occupied state. Our goal is to compute the Green's function $G(E)$ that is the inverse of a sparse matrix $D = E - \mathcal{H}$ of linear size $\sim N^2$. Clearly, a direct manipulation of the whole matrix is inefficient both in terms of time and storage, and becomes forbidding for $N > 100$. To circumvent this problem, we recursively decimate the irrelevant matrix elements of the Green's function. We start by decomposing Hilbert space into subspaces i , each of which is spanned by the states along one of the dashed lines in Fig. 1(a) and which are labeled by their dimensions $1 \leq i \leq N$. We denote the projection of D onto these subspaces as D_i . Clearly, D couples only neighboring subspaces (i) and ($i+1$), and we call the corresponding $[i \times (i+1)$ dimensional] coupling block in the Hamiltonian V_i . Finally, we define vectors $\mathbf{x}_i^{(n)}$ with elements

$$(\mathbf{x}_i^{(n)})_j = \langle N-i+j, j | G(E) | nn \rangle, \quad (9)$$

given by matrix elements of the Green's function G between a doubly occupied site $|nn\rangle$ and the states in subspace i . Since only neighboring subspaces are coupled, one readily derives from $DG = 1$ the set of coupled linear equations

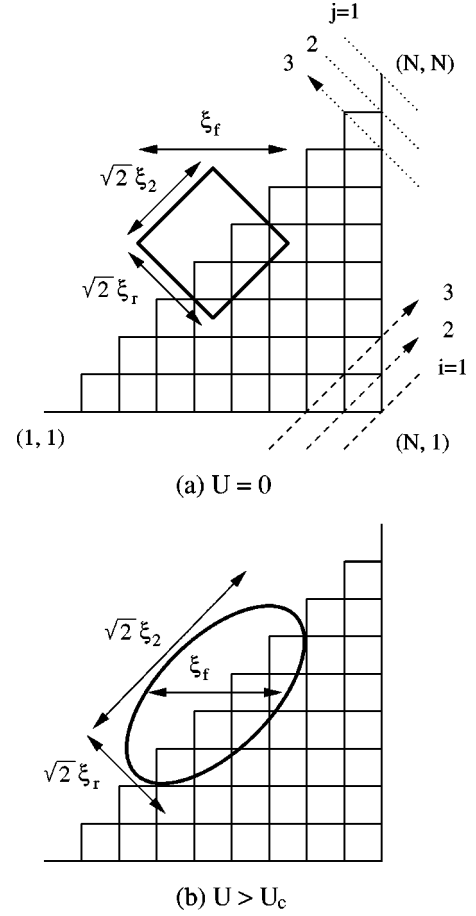


FIG. 1. Sketch of the two-dimensional lattice (thin solid lines) and the wave-function profile (thick solid lines). The dashed lines (dotted lines) represent the index scheme for the calculation of $\xi_{2,a}$ (ξ_r). Lengths are measured in terms of the lattice constant d . The factor $\sqrt{2}$ arises because ξ_r and ξ_2 are defined in units of the diagonal length of the smallest square of the lattice ($\sqrt{2}d$) while ξ_f is defined in units of its edge length (d).

$$D_1 \mathbf{x}_1^{(n)} + V_1 \mathbf{x}_2^{(n)} = 0,$$

$$V_{i-1}^T \mathbf{x}_{i-1}^{(n)} + D_i \mathbf{x}_i^{(n)} + V_i \mathbf{x}_{i+1}^{(n)} = 0, \quad 2 \leq i \leq N-1, \quad (10)$$

$$V_{N-1}^T \mathbf{x}_{N-1}^{(n)} + D_N \mathbf{x}_N^{(n)} = \mathbf{e}_n,$$

where \mathbf{e}_n is the N -dimensional unit vector with $(\mathbf{e}_n)_m = \delta_{n,m}$. Solving these equations, we obtain

$$\mathbf{x}_N^{(n)} = \mathcal{G}_N \mathbf{e}_n, \quad (11)$$

where the \mathcal{G}_i can be computed recursively from

$$\mathcal{G}_i = (D_i - V_{i-1}^T \mathcal{G}_{i-1} V_{i-1})^{-1} \quad \text{with } \mathcal{G}_1 = D_1^{-1}. \quad (12)$$

Finally noting that $(\mathbf{x}_N^{(n)})_i = \langle i | |G(E)| | nn \rangle$, we can now compute the localization length ξ_2 from Eq. (4). This reduces the calculation to manipulations of matrices of sizes from 1×1 to $N \times N$. It is worthwhile to point out that at the final stage of the iteration, the calculation is formally reduced to an effective 1D model for a single particle. It is straightforward to generalize the algorithm to compute the other localization lengths defined in this paper. For example, ξ_r is calculated by decomposing Hilbert space according to the dotted lines of Fig. 1(a).

For ξ_2 , we set $n=1$ in the above algorithm and obtain $t_{l,1} = \langle \langle \ln |\langle l|G|1\rangle| \rangle \rangle$ with $1 \leq l \leq N$ for each parameter set (W, U) . We find that $t_{l,1}$ depends linearly on l , implying an exponential decay of the Green's function. To eliminate finite-size effects near $l=1$ and $l=N$, we fit $t_{l,1}$ in the range $N/5 \leq l \leq 4N/5$ to

$$t_{l,1} = -\frac{l}{\xi_2} + c \quad (13)$$

with c a constant. We find that for chains $N \geq 200$, our results for ξ_2 are essentially independent of system size N , suggesting that finite-size effects on ξ_2 are rather weak. Similar procedures are performed for the other localization lengths.

Our main results are presented in Fig. 2. All data have been obtained for system size $N \geq 200$ and for the center of the band $E=0$. In view of the special nature of the doubly occupied sites due to the on-site interaction, it is natural to ask whether the definition for the two-particle localization length ξ_2 correctly captures the CM motion. To answer this question, we plot $\xi_{2,a}$ for interaction strength $U=1.0$ as function of a in Fig. 2(a). We find that $\xi_{2,a}$ remains unchanged up to rather large a , implying that ξ_2 is indeed a good description of the CM motion. In fact, $\xi_{2,a}$ remains independent of a even for $a > \xi_1$. Hence, as opposed to the previous beliefs^{2,5} the interaction affects the two-particle motion even if the particle distance exceeds ξ_1 . This can be understood in terms of single-particle propagation in the 2D lattice of Fig. 1. $\xi_{2,a}$ is associated with the transition probability along the dashed line a distance $\sim a$ from the diagonal. We recall that when $\langle m, m-a | G | n, n-a \rangle$ is expanded in powers of the hopping matrix element t , it is given by a sum over all possible paths from $|n, n-a\rangle$ to $|m, m-a\rangle$. If the distance between these two sites, $\sim |m-n|$, is much smaller than a , the effect of the interaction would be negligible. However, $\xi_{2,a}$ is defined by the limiting behavior of $|m-n| \rightarrow \infty$ with a finite, cf., Eq. (5). In this case, the contributions of paths that are sensitive to the interaction U are no longer negligible and $\xi_{2,a}$ remains influenced by the interaction even though $a > \xi_1$.

In Fig. 2(b), we show our results for ξ_r (symbols) that describes the decay of the Green's function with relative distance. For comparison, we also plot ξ_2 (lines). At $U=0$, the two lengths are equal within the numerical accuracy, i.e., $\xi_2 \approx \xi_r$. As U increases, ξ_r remains nearly constant while ξ_2 shows a pronounced enhancement in qualitative agreement with Shepelyansky's prediction.²

In Fig. 2(c) we plot ξ_f (symbols) and ξ_2 (lines), where the former describes the range over which one particle moves with the other one fixed. At $U=0$, we find that ξ_f approximately equals to $2\xi_2$. As already seen in Fig. 2(b), ξ_2 shows a strong increase with U . By comparison, ξ_f shows a much weaker increase. Hence, there exists a $U_c(W)$ beyond which ξ_2 exceeds ξ_f .

At $U=0$, the two particles move independently and the propagation of a given particle is not affected by whether the other is moving in the reverse (ξ_r) or in the same direction (ξ_2), implying $\xi_r = \xi_2$. Moreover, since ξ_2 measures two-particle propagation, while ξ_f the single-particle motion, one expects that the transition probability for ξ_2 is given by the square of that for ξ_f , so that $\xi_2 = \xi_f/2$. We note in passing

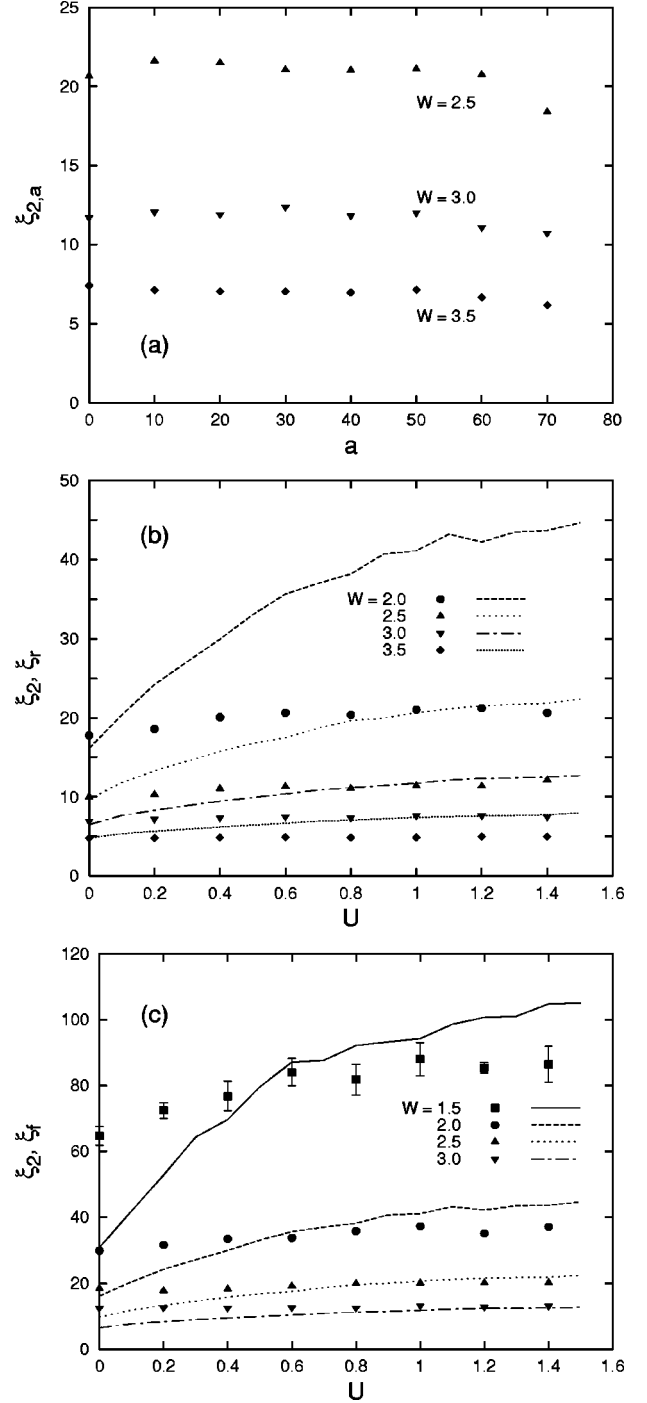


FIG. 2. (a) $\xi_{2,a}$ as function of a . (b) ξ_2 (lines) and ξ_r (symbols) as function of U . (c) ξ_2 (lines) and ξ_f (symbols) as function of U . All data have been obtained for system size $200 \leq N \leq 300$ and for $E=0$.

that $\xi_2(U=0) \neq \xi_1/2$, as was pointed out in Ref. 6. Since both ξ_r and ξ_f are determined by the limiting behavior for diverging distance between the particles, one does not expect them to be strongly influenced by the interaction. This explains the rather flat dependences of both lengths on U .

With the additional information from ξ_r and ξ_f , we can now construct a wave-function picture in the 2D lattice representation of the problem (Fig. 1). At $U=0$, this implies that the wave-function profile is described by a square as shown by a thick solid line in Fig. 1(a). As U increases, the

length of the edge associated with ξ_2 increases while that associated with ξ_r remains essentially constant. For $U > U_c$, the wave-function profile becomes highly anisotropic and we find that it can be well described by an ellipse as shown by the thick solid line in Fig. 1(b). The elliptical shape predicts the relation

$$\xi_f = \frac{2\xi_2\xi_r}{\sqrt{\xi_2^2 + \xi_r^2}}. \quad (14)$$

We have checked that our data are in good agreement with this expression for $U > U_c$. This clearly shows that the enhancement effect is associated predominantly with the direction of ξ_2 , i.e., the CM motion of the two particles.

These results allow us to resolve some of the above-mentioned discrepancies between previous numerical studies. We start by noting that the TMM measures the largest length scale from the N^2 Green's-function entries $\langle 1n|G|Nm\rangle$ with $1 \leq m, n \leq N$.⁸ According to our results, there are two competing lengths ξ_2 and ξ_f . For $U < U_c$, we find that the largest length is ξ_f while for $U > U_c$, it is ξ_2 . Therefore, the TMM actually measures ξ_f for $U < U_c$ and ξ_2 only for $U > U_c$. We first compare our results to those of Frahm *et al.*⁴ We find that their results for the localization length are two to three times larger than our result for $\max\{\xi_f, \xi_2\}$ at given values of W and U . We attribute this to large finite-size effects in the TMM, as suggested in Ref. 7. On the other hand, in Ref. 7, any enhancement effect was attributed to finite-size effects and it was suggested that the TMM produces the single-particle localization length for a sufficiently large system size. This is inconsistent with the

results of the present paper. We suggest the following explanation for the numerical results of Ref. 7. The argument of Ref. 7 is based on TMM data for $(W, U) = (3.0, 0)$ and $(3.0, 1.0)$ (restricting attention to short-range interaction). For $(W, U) = (3.0, 1.0)$, we find that the largest length is $\xi_f = 13.2 \pm 0.3$, which is close to $\xi_1 \approx 11.7$. Hence, we expect that the data in Ref. 7 in fact extrapolate to ξ_f , which is indistinguishable from ξ_1 within the numerical accuracy of Ref. 7. Analogous conclusion holds for $(W, U) = (3.0, 0)$. Therefore, we contend that the principal argument of Ref. 7 is a misinterpretation of data for a special parameter set and expect that the TMM exhibits the extrapolate to $\xi_2 \gg \xi_f$ which is indistinguishable from ξ_1 . Finally, we find that the ξ_2 's in Ref. 5 are somewhat larger than those in this paper, which we attribute to the approximate treatment of the Green's function in Ref. 5.

In summary, we have presented numerical results for various newly defined localization lengths of two interacting particles. It turns out that the enhancement effect exists mainly for the CM motion of the particles while both the relative motion and single-particle motion are only weakly dependent on the interaction strength. It has also been found that the enhancement effect for the CM motion is insensitive to the distance between the two particles beyond the single-particle localization length. Based on these results, a consistent explanation has been presented for the controversy in previous numerical studies.

We thank H. A. Weidenmüller for useful discussions. One of us (P.H.S.) has been partially supported by the Korea Science and Engineering Foundation.

¹S. V. Kravchenko, D. Simonian, M. P. Sarachik, W. Mason, and J. E. Furneaux, Phys. Rev. Lett. **77**, 4938 (1996).

²D. L. Shepelyansky, Phys. Rev. Lett. **73**, 2607 (1994); see also O. N. Dorokhov, Zh. Éksp. Teor. Fiz. **98**, 646 (1990) [Sov. Phys. JETP **71**, 360 (1990)].

³Y. Imry, Europhys. Lett. **30**, 405 (1995).

⁴K. Frahm, A. Müller-Groeling, J.-L. Pichard, and D. Weinmann, Europhys. Lett. **31**, 169 (1995).

⁵F. von Oppen, T. Wettig, and J. Müller, Phys. Rev. Lett. **76**, 491

(1996).

⁶P. H. Song and D. Kim, Phys. Rev. B **56**, 12 217 (1997).

⁷R. A. Römer and M. Schreiber, Phys. Rev. Lett. **78**, 515 (1997).

⁸K. Frahm, A. Müller-Groeling, J.-L. Pichard, and D. Weinmann, Phys. Rev. Lett. **78**, 4889 (1997); R. A. Römer and M. Schreiber, *ibid.* **78**, 4890 (1997).

⁹F. von Oppen and T. Wettig, Europhys. Lett. **32**, 741 (1995).

¹⁰P. Jacquod and D. L. Shepelyansky, Phys. Rev. Lett. **78**, 4986 (1997).